

NONDESTRUCTIVE EVALUATION AND MATERIALS CHARACTERIZATION USING
PHOTOTHERMAL-OPTICAL-BEAM-DEFLECTION IMAGING

G. C. Wetsel, Jr.* , J. W. Maclachlan** , J. B. Spicer** , and
J. C. Murphy

The Johns Hopkins University, Applied Physics Laboratory
Johns Hopkins Road, Laurel, MD 20707

INTRODUCTION

Photothermal-optical-beam-deflection (PTOBD) imaging involves use of a focused, modulated laser beam to locally heat a sample and a second laser beam to probe the resulting changes in sample temperature. For opaque samples, the photothermal heating occurs essentially at the surface and temperature changes in the bulk occur via thermal diffusion to a depth below the surface of the order of a thermal-diffusion length, $\delta = (2\kappa/\rho C\omega)^{1/2}$, where κ is the thermal conductivity, ρ is the density, C is the specific heat, and ω is the modulation frequency. Since the limiting factor in definition/resolution is not the thermal diffusion length [1,2], features of the order of the heating-laser-beam diameter or smaller can be investigated, even at relatively low modulation frequencies. Lateral spatial resolution for subsurface features much closer to the surface than a diffusion length is independent of the diffusion length and is determined principally by the diameter of the heating beam, although the diameter of the probe beam can affect the resolution [1-4]. Generally, the limiting factors on spatial resolution in PTOBD imaging are the heating-beam diameter, the shape and depth of the subsurface feature being imaged, and the modulation frequency (to a lesser extent) [2,4]. This paper presents images of a number of important classes of materials with resolution less than 10 μm . Some contrast issues and underlying materials issues are discussed qualitatively.

The PTOBD images are formed by measuring the deflection of a He-Ne probe-laser beam caused by an Ar^+ -laser heating beam scanning the sample [5]. The diameter of the heating beam is estimated to be about 5 μm . The probe beam was unfocused in these experiments and had a diameter of approximately 0.8 mm. Both the amplitude and phase of the normal and transverse deflection signals were measured using an EGG Princeton Applied Research 5301 dual channel lockin amplifier. In this paper these images are presented using a 16 level gray scale. Control of the experiment was provided by a HP 9836C computer [6].

DISCUSSION

PTOBD images of a polished specimen of 2024 aluminum are shown in Figures 1-3. Image detail of a few microns is clearly resolved. This scale is commensurate with the 1 μm step size of the translators moving the

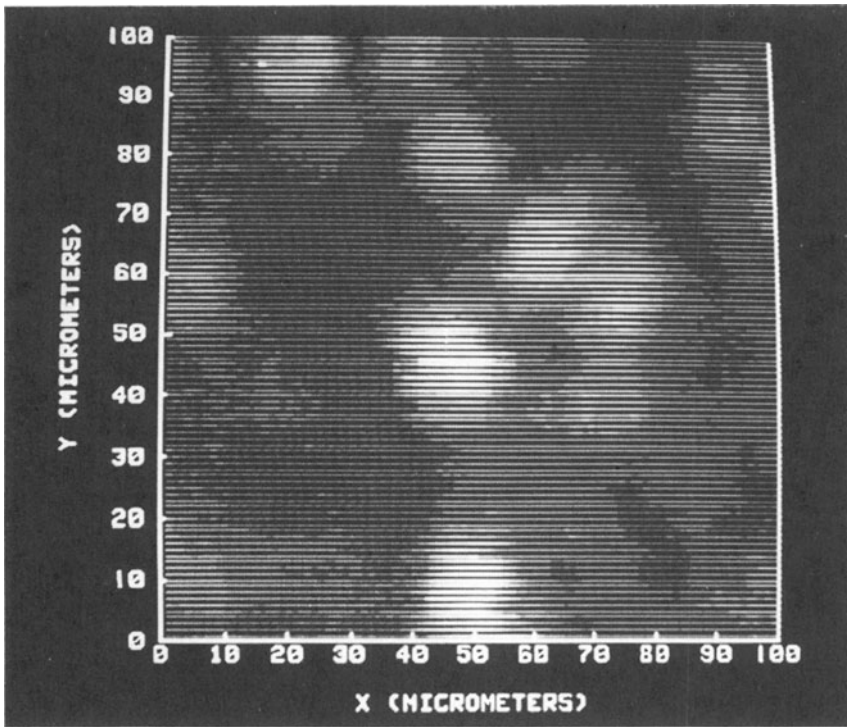


Fig. 1. Normal PTOBD amplitude image of sample of 2024 aluminum, $f = 2$ kHz.

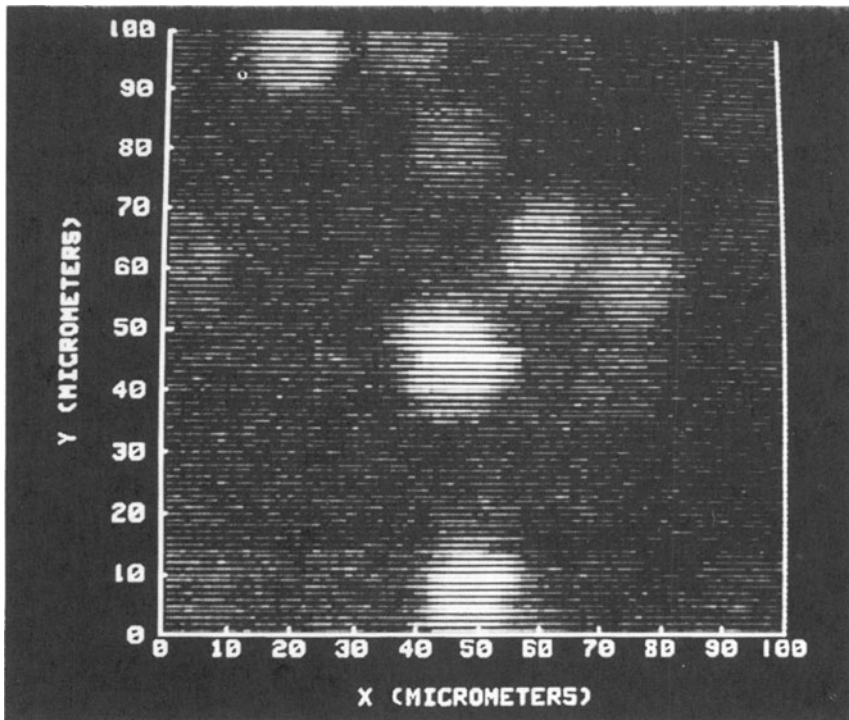


Fig. 2. Normal PTOBD phase image of sample of 2024 aluminum, $f = 2$ kHz.

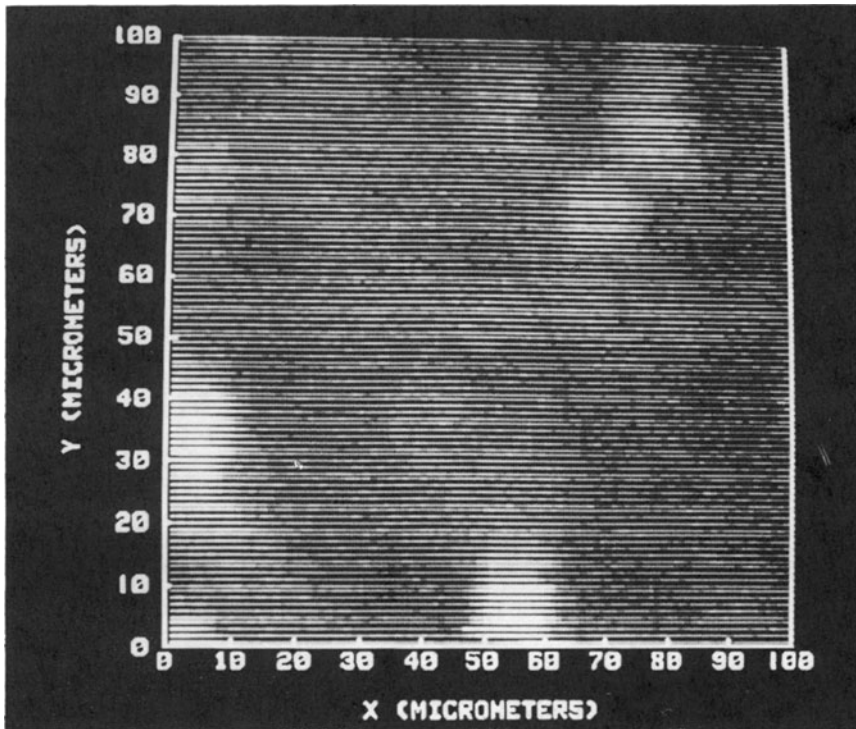


Fig. 3. Transverse PTOBD amplitude image of sample of 2024 aluminum, $f=2$ kHz.

specimen and with the estimated diameter of the Ar^+ pump beam. Note that since the amplitude image (Fig. 1) and the phase image (Fig. 2) show similar structure, thermal contrast, not optical contrast, is the basis of the images observed. Notice also that the transverse PTOBD image (Fig. 3) is strikingly different from the normal image. Optical and SEM micrographs and SEM/EDAX (energy dispersive X-ray analysis) images have also been made for this sample. They reveal the presence of inclusions associated with iron and manganese impurities within the aluminum matrix. The geometric scale of these inclusions is approximately $10\ \mu\text{m}$ in linear aspect consistent with the PTOBD feature sizes. We tentatively associate inclusions with the PTOBD contrast observed in Figs. 1-3. The issue of how coherent these inclusions are with the matrix has not yet been resolved. This question and the associated question of the relationship of coherency and thermal boundary impedance are important issues for future study. They may be connected with the differences observed between normal and transverse images.

Figures 4 and 5 show normal OBD images of a refractory Ni-based alloy covered with a diffusion-bonded aluminum coating. Again, the images show micrometer-scale thermal features as well as features which, while of the same geometric size, are clearly of optical origin. The microstructural basis of the PTOBD image features has not been unambiguously determined at this time. However, SEM micrographs of the interface of other samples in this series indicate that the coating penetrates the substrate with long "fingers" whose cross-section approximates $10\ \mu\text{m}$. The size of these features of the interface corresponds to the image features observed and suggests that the thermal features in the PTOBD image are representations of the subsurface fingers.

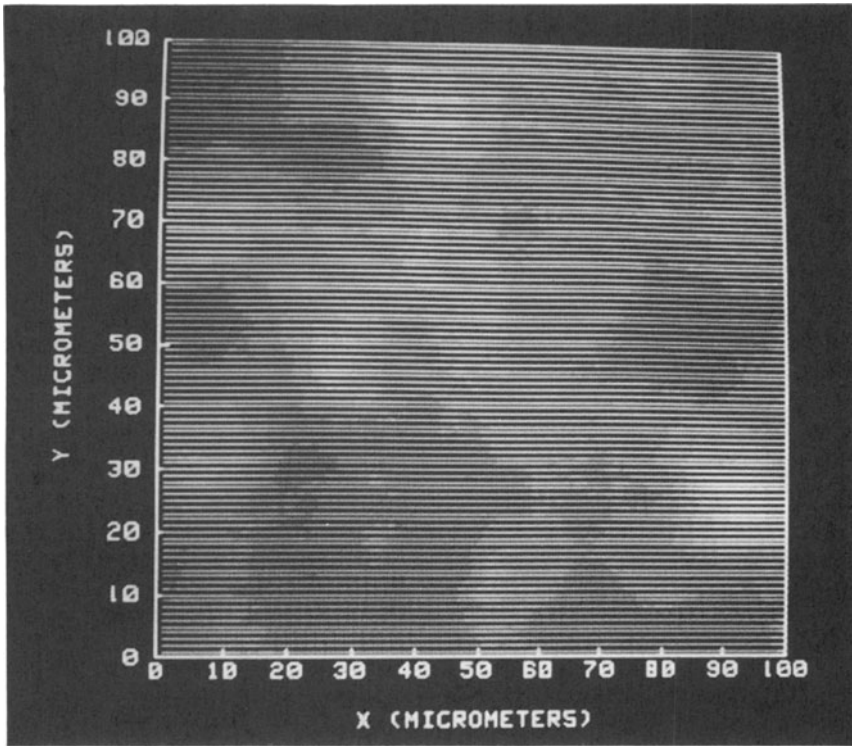


Fig. 4. Normal PTOBD amplitude image of sample with diffusion-bonded coating, $f = 500$ Hz.

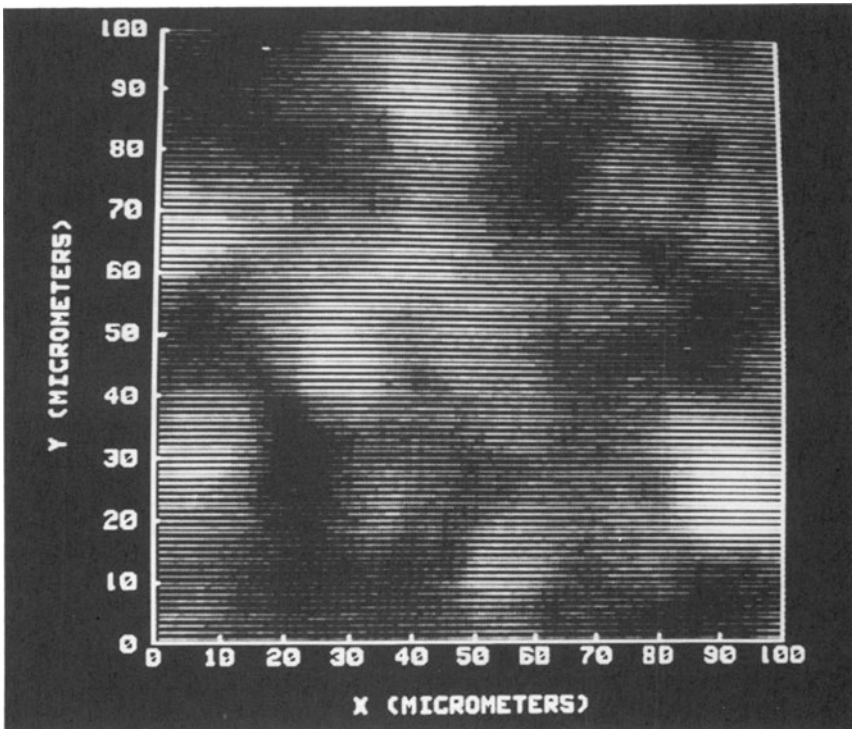


Fig. 5. Normal PTOBD phase image of sample with diffusion-bonded coating, $f = 500$ Hz.

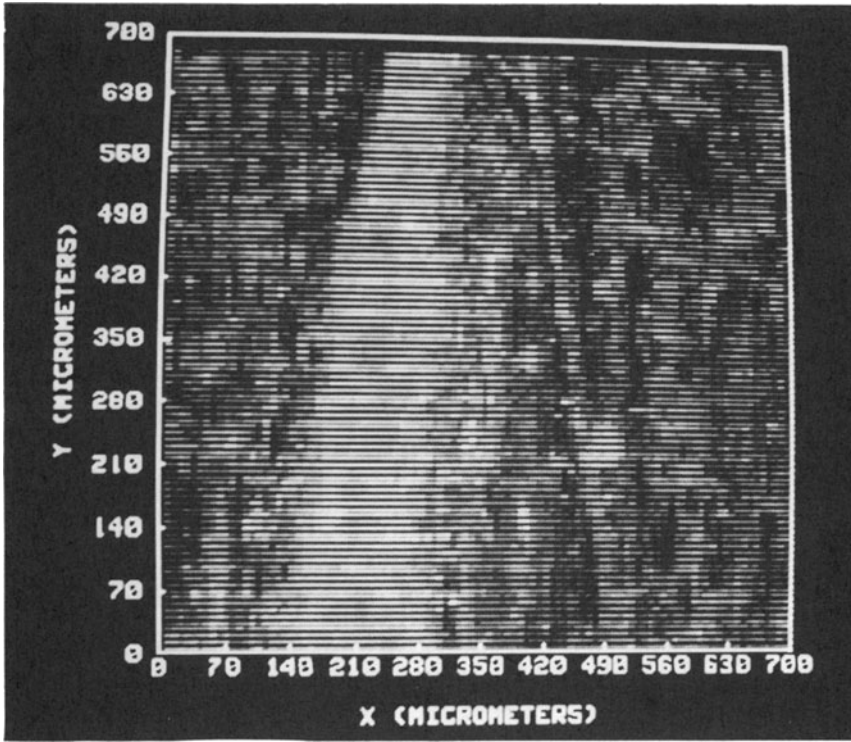


Fig. 6. Normal PTOBD amplitude image of sample of graphite-aluminum composite material, $f = 200$ Hz.

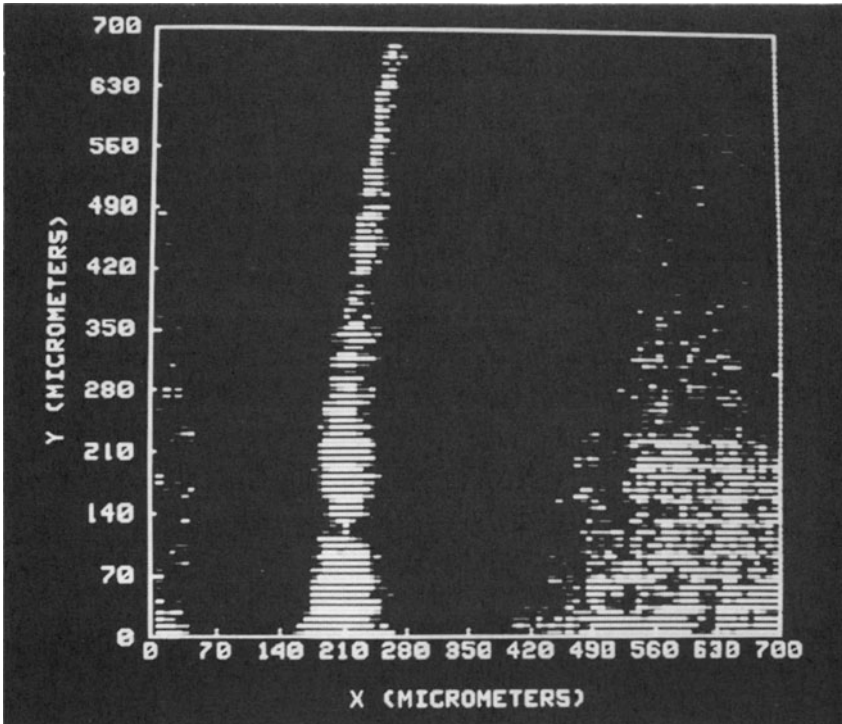


Fig. 7. Normal PTOBD phase image of sample of graphite-aluminum composite material, $f = 200$ Hz.

Normal-deflection PTOBD amplitude and phase images of a unidirectional graphite aluminum composite are shown in Figures 6 and 7. This specimen had breaks in the aluminum coatings parallel to the fiber direction which presumably occurred through differential contraction during fabrication. In the PTOBD images contrast is seen at the break and in regions on either side of the visual break. The extension of the PTOBD contrast beyond the visual region may be related to changes in the fiber-aluminum bond caused by stress. In other studies on this material using scanning electron acoustic techniques (SEAM), periodic "puckers" were observed on a line orthogonal to the break direction. These also suggested local regions of directed internal stress. In the SEAM experiments the largest break opening was coincident with the location of the "puckers".

As a final example of PTOBD applications, Figure 8 is a transverse deflection scan of a grain boundary in a high-purity aluminum bicrystal. The sample was grown from the melt using two separated seeds. The resulting crystals were allowed to have a common interface in the melt at a point above the seeds. X-ray topographic analysis has shown that each region is single crystalline with some substantial lattice distortion occurring at points parallel to the grain boundary. For the PTOBD studies, the specimen was first mechanically polished and subsequently chemically polished. The sample was intentionally somewhat overetched to make the boundary visible for image registration purposes. The scan shown in Figure 8 represents 200, 1.6 micron steps. For this case a focused probe beam was used with estimated diameter of 0.07 μm .

Figure 8 shows an amplitude minimum at the grain boundary. On either side of the boundary there are relative maxima whose amplitudes depend weakly on frequency in the range 250-4000 Hz. Similar results were obtained for the normal PTOBD scans. This signal variation is characteristic of the temperature dependence predicted for a thermally insulating plane

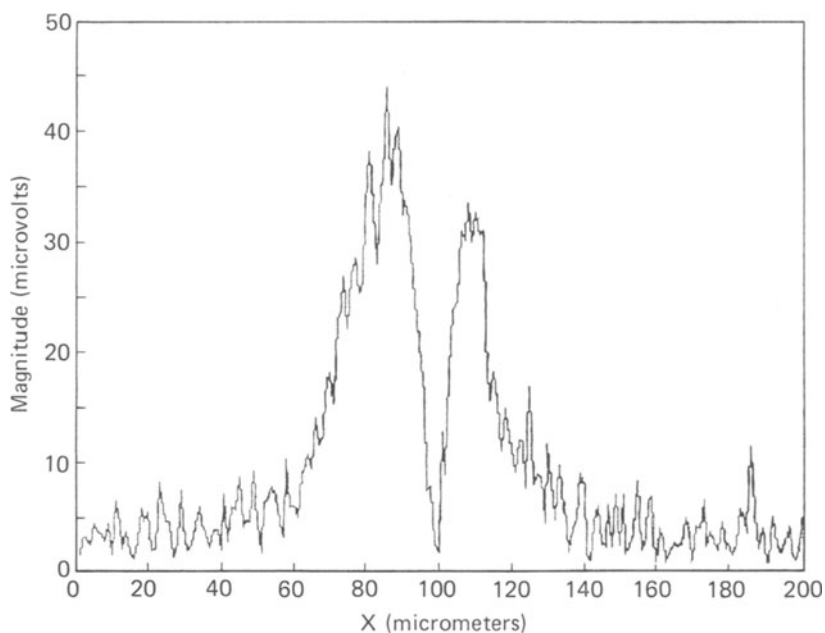


Fig. 8. Transverse PTOBD amplitude vs. X for aluminum bicrystal in neighborhood of grain boundary, $f = 2 \text{ kHz}$

perpendicular to the sample surface that inhibits heat flow parallel to the surface of the sample. For a scanned point excitation source, a temperature increase on either side of the insulating boundary occurs [2] as the source approaches the boundary. Both normal and transverse scans also show evidence of subsurface structure. Similar evidence of near boundary structure has been developed in SEAM imaging of the same specimen. Significantly, the PTOBD signal varies in amplitude along the interface. On occasion the boundary is not observed. This is in contrast to the SEAM scans where the boundary is always seen, although with varying spatial signature. This suggests that the observed PTOBD signal is associated with spatial variations in the thermal impedance of the grain boundary, possibly related to the presence of lattice deformation or to impurities at the interface. It then appears that a modification of the temperature distribution by thermal properties associated with the interface between two crystals has been observed. However, the contrast between the PTOBD and acoustic detection imaging methods leaves questions of the nature of the mechanisms yet unresolved.

In summary, PTOBD methods are sensitive, relatively high resolution probes of specimen microstructure which are applicable to a wide range of specimens.

REFERENCES

* Permanent address: Department of Physics, Southern Methodist University, Dallas, TX 75275

** Permanent address: Department of Materials Science and Engineering, The Johns Hopkins University, Baltimore, MD 21218

1. G. C. Wetsel, Jr. and F. A. McDonald, *J. Appl. Phys.* 56, 3081 (1984).
2. F. A. McDonald and G. C. Wetsel, Jr., "Resolution and Definition in Thermal Imaging," 1984 IEEE Ultrasonics Symposium Proceedings, pp. 622-628, IEEE, New York (1984).
3. L. C. Aamodt and J. C. Murphy, *J. Appl. Phys.* 52, 4903 (1981).
4. F. A. McDonald, G. C. Wetsel, Jr., and G. E. Jamieson, "Spatial Resolution of Subsurface Structure in Photothermal Imaging," in Acoustical Imaging, Vol. 14, Plenum, London (1985).
5. L. C. Aamodt and J. C. Murphy, *Appl. Opt.* 21, 111 (1982).
6. F. A. McDonald, G. C. Wetsel, Jr., and S. A. Stotts, "Scanned Photothermal Imaging of Subsurface Structure," Acoustical Imaging, Vol. 12, pp. 147-155, E. A. Ash and C. R. Hill, Ed., Plenum, London (1982).